Determining contact potential barrier effects on electronic transport in single molecular junctions

Jianfeng Zhou and Bingqian Xu

Citation: Appl. Phys. Lett. **99**, 042104 (2011); doi: 10.1063/1.3615803
View online: http://dx.doi.org/10.1063/1.3615803
View Table of Contents: http://aip.scitation.org/toc/apl/99/4
Published by the American Institute of Physics

Determining contact potential barrier effects on electronic transport in single molecular junctions

Jianfeng Zhou and Bingqian Xu[a)]
Single Molecule Study Laboratory, Faculty of Engineering and Nanoscale Science and Engineering Center, University of Georgia, Athens, Georgia 30602, USA

(Received 19 April 2011; accepted 4 July 2011; published online 27 July 2011)

The authors introduced a simplified multiple-barrier model based on the widely accepted traditional tunneling model to describe the electron transport behaviors in single molecule junction systems. The contact potential barrier height Φ_c and the contact decay constant β_c were taken as the key indexes to represent certain contact conformations. By monitoring the dynamic changes of contact potential barriers corresponding to the mechanical extension of contact conformations with our newly developed Scanning Probe Microscope (SPM)-break junction technique and then fitting into the model, we established an in-depth and detailed understanding of the molecule-metal contact effects on electronic transport properties in single molecular junctions. © *2011 American Institute of Physics*. © *2011 American Institute of Physics*. [doi:10.1063/1.3615803]

The fundamental understanding of electron transport mechanisms in single molecular junctions is crucial to construct molecular junction devices.[1] The main efforts on electron transport properties of molecular junction are focused on identifying the main factors involved in the electron transport process.[2] Simply speaking, the conductance G of molecular junctions at low bias follows the Landauer-Büttiker Formalism and can be put as[3]

$$G = \frac{2e^2}{h} T_{LC} \cdot T_{MOL} \cdot T_{RC}, \tag{1}$$

where T_{MOL} is the molecule transmission efficiency, which reflects the molecule backbone contribution to the electronic transport. T_{LC} and T_{RC} are the contact transmission efficiencies of charge transport across the left and right contacts in molecular junctions. In most cases, these three parameters couple with each other to become so complex that they cannot be interpreted analytically in simple formations. Therefore, more advanced theoretical and computational tools, such as density functional theory (DFT) and non-equilibrium Green function (NEGF),[4] were used to discuss these three transmission efficiencies. However, the theoretical results usually cannot directly compare with experimentally measured quantities. For specific molecular junctions, such as N-alkane molecule with large HOMO-LUMO gap, the dominant charge transport mechanism normally follows coherent and non-resonant tunneling.[5] In this so called Simmons tunneling model, the molecular core can be considered as a rectangular barrier and T_{MOL} is exponentially decreasing with the width of the barrier or the length of the molecule l

$$T_{MOL} = \exp(-\beta l) \tag{2}$$

Molecular decay constant, β, is a significant parameter used to describe the electron transport properties of molecule core.

While most researches mainly focused on the influences of molecule core on the electron transport in molecular junctions,[6] recent experimental and theoretical results[7,8] indicate that molecule-metal contacts in molecular junctions play important and even crucial roles. Variations of contact conformations usually result in totally different transport behavior.[9] Unfortunately, the experimental difficulties to obtain more complete details of the contact conformations in molecular junctions greatly hinder such efforts.[7,10]

It was recently found that an applied external mechanical modulation can modify the contact conformations of molecular junctions and cause the changes of electron transport properties of molecular junctions.[11] However, a complete picture is needed to bridge the experimental results with the fundamental understanding of how the contact potential barriers impact the electronic transport behaviors. In this letter, we try to extend the traditional Simmons tunneling model and fit our measured data to discuss the contacts impact on the electron transport behavior of single molecular junctions in detail.

We used a multiple rectangular barrier model[12] to represent the molecule core and contacts, respectively (Figure 1), which the conductance of the molecule junction can be written as

$$\begin{aligned} G &= A\exp(-\beta_C d_{LC})\exp(-\beta l)\exp(-\beta_C d_{RC}) \\ &= A\exp(-\beta l)\exp(-\beta_C d_C), \end{aligned} \tag{3}$$

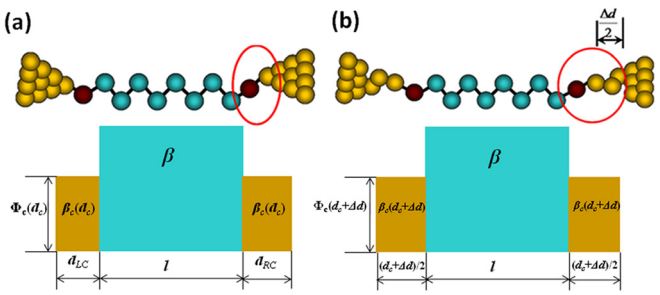

FIG. 1. (Color online) The schematics of energy profile (a) without and (b) with the extension Δd of molecular junctions in contacts. The circles label the contact conformation changes. d_c is the width of contact barrier without extensions of molecular junctions, and l is the length of the molecule. β and β_C are decay constants of the molecule and contact, respectively.

[a)]Electronic mail: bxu@engr.uga.edu.

where A is a constant. In this model, the measured conductance also shows exponential decrease with the contact rectangular barrier width. The left contact barrier with barrier width d_{LC} and the right contact barrier with barrier width d_{RC} can be combined into one potential barrier with width d_C. The contact decay constant β_C is determined by the contact potential barrier height Φ_C. Thus, we can conclude that the changes of contact conformation can be completely revealed by determining these two parameters of the contact potential barrier. Furthermore, when the molecule core keeps intact, the measured conductance changes of molecular junction could be determined by the detailed features, such as height, width or both of contact potential barriers. It is worthy noticing that in analysis of individual molecular junctions under extensions in real experiments, the symmetric assumptions are definitely too simple for the discussions. However, there is no way of controlling the contact configuration of individual junctions experimentally, and therefore, it is not possible to analyze such individual single junctions. Therefore, although in the real experiments, the individual molecular junctions could show asymmetric contact structure under extension, the averaged results of hundreds of molecular junctions should show symmetric conformations under the similar extensions.

Single 1,8-octanedithiol (C8DT) molecular junctions were formed with SPM break junction technique, and mechanical modulations were applied to extend and press but not break the wired molecular junctions.[11,13,20] Here, the 0.6 Å modulation amplitude was used for the discussion to avoid possible junction breaking or switching between different contact conformations at higher modulation amplitudes as is discussed in our previous report.[11] As the applied mechanical extensions were found to mainly modify the conformations of contacts but not the molecule core,[11] the induced changes of contact conformations would result in contact potential barrier changes as shown in Figure 1, which would finally alter the electron transport behavior in molecular junctions. Therefore, we take the displacement of external extensions Δd to represent the width changes of the contact barrier. In real systems, the heights of contact potential barrier should also be altered under the external mechanical extension and, therefore, influences single molecular conductance. The contact decay constant β_C and contact potential barrier height Φ_C can then be deduced from Eq. (3) (Ref. 20)

$$\beta_C(d) = -\frac{\partial \ln(G)}{\partial(d)} \quad \text{and} \quad \Phi_C(d) = (1/1.03)\left(\frac{\partial \ln(G)}{\partial(d)}\right)^2, \tag{4}$$

which can be calculated from the measured conductance (G) change and displacement (d). As is shown in Figure 2(a), we monitored the changes of single C8DT molecular junction conductance while changing the junction extensions by applying regular mechanical modulations. By re-plotting the conductance changes versus mechanical extensions of parts of curves indicated in the rectangular box in Figure 2(a), we obtained the conductance-extension curves shown in Figure 2(b). Without any mechanical extension, the conductance of single free-holding C8DT junction is found to be around $2.5 \times 10^{-4} G_0$, agreeing well with previously reported results.[14] The conductance of molecular junction decreased as the molecular junctions were extended by SPM tip (Figure 2(b)). However, as is shown in Figure 2(b), $\ln(G/G_0)$ does not decrease exactly linearly with extension or width changes of contact barrier. It indicates that during the extension, β_C changes or Φ_C changes or both change. From Eq. (4), we obtained the contact decay constant at different extension distances (Figure 2(c)). The results using individual curves demonstrated that for C8DT molecular junctions, the contact decay constant will roughly increase with the extensions but differs for individual curves. Therefore, to obtain the overall trend, we did statistics analysis using more than 200 conductance-extension curves of single C8DT molecular junctions obtained in our experiments. The histograms of contact decay constant β_C at certain extension distances were constructed as is shown in Figure 3. In Figure 3(a), it shows the histogram of β_C without any extension. From this histogram, the peak value of the Gauss fitting is taken as the most probable value of β_C for free-holding C8DT molecular junction, which is found to be around 0.115 ± 0.035 Å^{-1}. This value is close to the results reported previously by using other experimental technique.[12] Remarkably, this value is far smaller than the molecular decay constants of C8DT molecule core (around 0.8 Å^{-1}).[14,15] Thus, the strong Au-thiol bonds do provide relative low contact resistance for the molecular junctions.

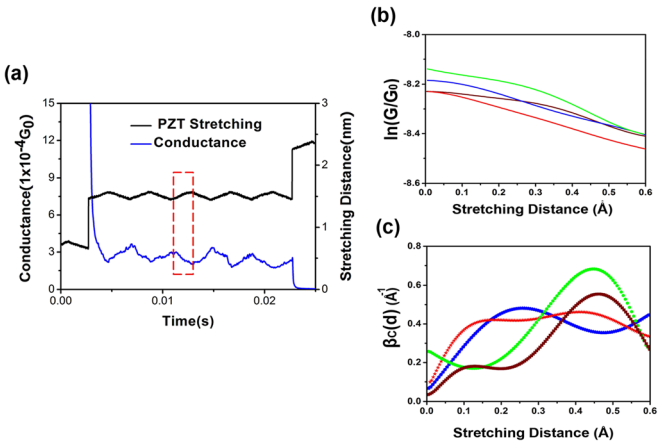

FIG. 2. (Color online) (a) A typical conductance trace under the mechanical modulations. The highlighted curves by the rectangular box show the conductance changes under the extensions; (b) Four representative curves show the conductance changes with extension distance; and (c) The contact decay constant β_C changes under extension distance obtained from the curves in (b).

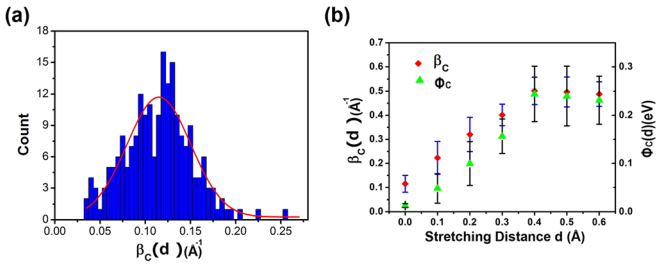

FIG. 3. (Color online) (a) Histograms of contact decay constant $\beta_C(d_c)$ in C8DT junction without extensions (from around 200 curves); (b) Contact decay constant $\beta_C(d)$ changes and contact barrier height $\Phi_C(d)$ with extension distance d. The curve in (a) is the Gaussian fitting of the statistical histogram and the value of each point in (b) Gaussian fitting center of histogram at certain stretching distance obtained by the similar statistical methods. The standard deviations, the full widths at half-maximum (fwhm) histogram peak from the Gaussian fitting are marked as the error bars in (b).

Figure 3(b) plots the histogram determined β_C under different extension d, which shows that at small extension d, β_C of C8DT molecular junctions increase linearly with SPM probe stretching. However, after extension d becomes larger than 0.4 Å, the contact decay constants β_C keeps around 0.5 $Å^{-1}$ (the contact barrier heights Φ_C keeps around 0.25 eV) and do not show obvious change with further extension. Here, we provide a possible explanation for this behavior. The contacts in molecular junctions include not only the contact bond between the end group of the molecule and the metal atom but also the bonds between metal atoms close to the contact bond.[16] Therefore, any changes of these bonds will affect the electron transport, for example, the extension of the bonds will contribute to the increase of the contact barrier width and therefore decrease the transmission efficiency. In the C8DT molecular junctions, the thiol–Au bond is stronger than the Au–Au bond, so the extensions cause the rearrangement of gold atoms in contacts, which results in increases of distance among atoms and the reconstructions of electronic potential profiles in the contacts.[16] The decrease of single molecular junction conductance under extension, therefore, was caused by both redistribution of potential energy and continuous increasing width of contact potential barrier. However, after the extension reaches a certain distance (0.4 Å), the contact gets to a metastable configuration, where the further increase of the distance between atoms in contacts will not cause noticeable changes of the distributions of electronic potential. Therefore, the further decrease of single molecular junction conductance after more than 0.4 Å extension should be only due to the increasing width of contact potential barrier.

To further understand different dynamic changes of contact potential barrier under different contact configurations, we also investigate single 1,8-octanediamine (C8DA) molecular junctions with NH_2–Au bond in the contacts instead of thiol–Au bond in C8DT junctions. In this case, $\ln(G/G_0)$ decreases roughly linearly with extension (Figure 4(a)). The contact decay constant β_C of C8DA junctions without extensions is determined to be 0.374 ± 0.105 $Å^{-1}$(Figure 4(b)), much greater than that of C8DT junctions. The weaker coupling of amine–Au bond in the contact should be also responsible for both greater β_C and Φ_C in the C8DA molecular junctions even without any mechanical extension. The higher heights but similar width of contact barrier (thiol–Au and amine–Au have similar bond length[17]) could also explain the smaller measured single molecular conductance of C8DA junctions ($5.2 \times 10^{-5} G_0$) comparing to that of C8DT molecular junctions under the same experiment conditions.[18] Furthermore, the contact decay constant of C8DA junctions show less dependence on the extension distances (Figure 2(b)), indicate that the applied external mechanical extension is not big enough to cause the reorganization of gold atomic configurations because amine–Au bond is weaker than the Au–Au bond.[19] The extension of contact can be attributes to the distance changes in amine–Au bond but cannot lead to distortion in contacts with redistribution of gold atoms as is in C8DT molecular junctions. Therefore, the width of contact potential barrier is still modified by the extensions of C8DA molecular junctions while the height of contact potential barrier is not sensitive to the extensions anymore. Comparing the results for C8DT and C8DA molecular junctions obtained by fitting the simple model with the measured conductance and mechanical extensions, we clearly demonstrated that conductance differences of molecular junctions with the same molecule core are induced by different contacts. However, detailed and strict descriptions about how the contact potential changes with contact conformations is an extremely complicated issue and need more improved theoretical and experimental discussions.

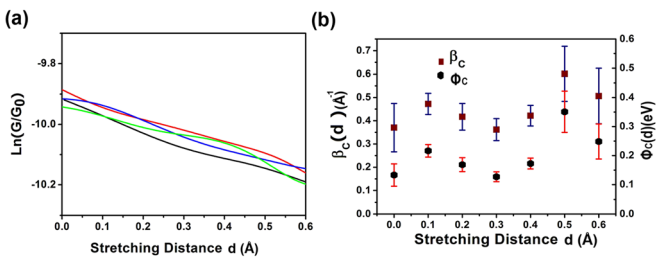

FIG. 4. (Color online) (a) Representative conductance-extension curves of C8DA and (b) contact decay constant $\beta_C(d)$ changes and height changes of contact potential barrier $\Phi_C(d)$ in C8DA molecular junctions with extension distance d.

In summary, we have investigated the influences of contact conformation changes on the electron transport in molecular junctions by introducing a multiple-barrier tunneling model and fitting the measured data. This approach could bridge the current experimental results with the fundamental understanding of conduction mechanism in the single molecular junctions.

We gratefully acknowledge National Science Foundation (ECCS 0823849) for financial support.

[1]N. J. Tao, Nat. Nanotechnol. **1**, 173 (2006).
[2]A. Nitzan and M. A. Ratner, Science **300**, 1384 (2003); S. M. Lindsay, Electrochem. Soc. Interface Spring, **26** (2004).
[3]H. B. Akkerman and B. de Boer, J. Phys.: Condens. Matter. **20**, 013001 (2008).
[4]Y. Qi, J. Qin, G. Zhang, and T. Zhang, J. Am. Chem. Soc. **131**, 16418 (2009); F. Evers, F. Weigend, and M. Koentopp, Phys. Rev. B **69**, 235411 (2004); X. Y. Feng, Z. Li, and J. Yang, J. Phys. Chem. C **113**, 21911 (2009).
[5]T. Lee, W. Wang, and M. A. Reed, Ann. N.Y. Acad. Sci. **1006**, 21 (2003); J. M. Beebe, V. B. Engelkes, J. Liu, J. J. Gooding, Paul K. Eggers, Y. Jun, X. Zhu, M. N. Paddon-Row, and C. D. Frisbie, J. Phys. Chem. B **109**, 5207 (2005).
[6]A. Aviram and M. A. Ratner, Chem. Phys. Lett. **29**, 277 (1974); C. A. Mirkin and M. A. Ratner, Annu. Rev. Phys. Chem. **43**, 719 (1992).
[7]S. M. Lindsay, Faraday Discuss. **131**, 403 (2006).
[8]S. M. Lindsay, J. Chem. Educ. **82**, 727 (2005).
[9]J. A. Malen, P. Doak, K. Baheti, T. D. Tilley, R. A. Segalman, and A. Majumdar, Nano Lett. **9**, 1164 (2009); H. Liu, N. Wang, J. Zhao, Y. Guo, X. Yin, F. Y. C. Boey, and H. Zhang, Chem. Phys. Chem. **9**, 1416 (2008).
[10]S. M. Lindsay and M. A. Ratner, Adv. Mater. **19**, 23 (2007).
[11]J. Zhou, G. Chen, and B. Xu, J. Phys. Chem. C **114**, 8587 (2010).
[12]G. Wang, T. Kim, H. Lee, and T. Lee, Phys. Rev. B **76**, 205320 (2007).
[13]B. Xu, Small **3**, 2061 (2007).
[14]B. Xu and N. J. Tao, Science **301**, 1221 (2003).
[15]S. Jang, P. Reddy, A. Majumdar, and R. A. Segalman, Nano Lett. **6**, 2362 (2006).
[16]K.-H. Müller, Phys. Rev. B **73**, 045403 (2006).
[17]G. Peng, M. Strange, K. S. Thygesen, and M. Mavrikakis, J. Phys. Chem. C **113**, 20967 (2009).
[18]J. Zhou, F. Chen, and B. Xu, J. Am. Chem. Soc. **131**, 10439 (2009).
[19]Z. Li and D. S. Kosov, Phys. Rev. B **76**, 035415 (2007).
[20]See supplementary material at http://dx.doi.org/10.1063/1.3615803 for experimental details and the derivations of contact decay constant and contact potential height.